

Image-based Compensation for Involuntary Motion in Weight-bearing C-arm Cone-beam CT Scanning of Knees

Mathias Unberath^{a,b}, Jang-Hwan Choi^a, Martin Berger^{a,c}, Andreas Maier^b, Rebecca Fahrig^a
^aDepartment of Radiology, Stanford University, Stanford, CA 94305; ^bFriedrich-Alexander
University Erlangen-Nuremberg, 91058 Erlangen, Germany; ^cGraduate School Heterogeneous
Image Systems, FAU Erlangen-Nuremberg, Germany;

ABSTRACT

We previously introduced four fiducial marker-based strategies to compensate for involuntary knee-joint motion during weight-bearing C-arm CT scanning of the lower body. 2D methods showed significant reduction of motion-related artifacts, but 3D methods worked best.

However, previous methods led to increased examination times and patient discomfort caused by the marker attachment process. Moreover, sub-optimal marker placement may lead to decreased marker detectability and therefore unstable motion estimates. In order to reduce overall patient discomfort, we developed a new image-based 2D projection shifting method.

A C-arm cone-beam CT system was used to acquire projection images of five healthy volunteers at various flexion angles. Projection matrices for the horizontal scanning trajectory were calibrated using the Siemens standard PDS-2 phantom. The initial reconstruction was forward projected using maximum-intensity projections (MIP), yielding an estimate of a static scan. This estimate was then used to obtain the 2D projection shifts via registration.

For the scan with the most motion, the proposed method reproduced the marker-based results with a mean error of 2.90 mm \pm 1.43 mm (compared to a mean error of 4.10 mm \pm 3.03 mm in the uncorrected case). Bone contour contrast as well as the continuity of the surrounding modeling clay layer was improved. The proposed method is a first step towards automatic image-based, marker-free motion-compensation.

Keywords: weight-bearing knee, image-based motion compensation, C-arm cone-beam CT, motion artifacts, fiducial marker, mutual information, medical image processing

1. INTRODUCTION

Recent advances in cone-beam Computed Tomography (CBCT) allow for the image acquisition of joints under weight-bearing conditions [1,2]. This is of particular interest in weight-bearing knee joint imaging, as knee joint kinematics under weight-bearing conditions have been shown to differ from those in supine positions. Thus, imaging patients *in vivo* under weight-bearing conditions might lead to improved diagnoses regarding knee cartilage health [3]. Additionally, C-arm CBCT scanners have flexible imaging trajectories as well as wide volumetric beam coverage, enabling the system to image both knees simultaneously [1,2].

Images acquired under weight-bearing conditions, however, are susceptible to severe motion artifacts because involuntary knee motion is common during data acquisition. Our previous studies required the use of fiducial markers, which were used in four different correction methods in two dimensions (2D projection shifting, 2D projection warping) or three dimensions (3D image warping and 3D iterative image warping) for involuntary motion compensation [1,4]. The 3D methods worked best because they were able to more accurately describe the effects of involuntary lower body motion on the projections. Nevertheless, the more restricted 2D projection shifting approach also significantly reduced motion-related artifacts [1,4].

However, all previously proposed methods require the attachment of fiducial markers to the patient's knees. The marker placement is crucial, as the detection of sub-optimally placed markers can be challenging. Incorrect estimates of the marker location can lead to less accurate involuntary motion estimates [4]. Additionally, the marker attachment

procedure leads to longer preparation times for the examination and increase overall patient discomfort. To overcome the need for fiducial markers, we propose an image-based 2D projection-shifting algorithm. The method uses MIPs of an initial, uncompensated reconstruction, and 2D shifts are obtained by registering the initial projections to the forward-projected reference.

2. MATERIALS AND METHODS

Five healthy volunteers were imaged squatting with different knee flexion angles using a C-arm cone-beam CT system (Axiom Artis dTA, Siemens AG, Forchheim, Germany) with a flat panel detector. The tube voltage was 70 kVp, and the detector dose was 1.2 $\mu\text{Gy}/\text{frame}$. A total of 248 frames were acquired over π plus the fan angle in 10 seconds. Each projection had 1240 x 960 pixels with an isotropic resolution of 0.308 mm after 2 x 2 binning. Nine tantalum markers were attached around both knees. A layer of modeling clay was wrapped around both legs to prevent detector saturation artifacts. A geometrical calibration for the horizontal C-arm trajectory was obtained using the PDS-2 phantom, generating 248 projection matrices $P = \{P_i\}_{i=1}^n$ [2].

All images were reconstructed using the following procedure: automatic exposure control compensation [5], low contrast water correction [6], dynamic density optimization scatter correction [7], cosine-weighting [8], Parker redundancy weighting [9], truncation correction [10], ramp filtering using a modified Shepp-Logan kernel with roll-off [8] (cutoff frequency: 0.73 cycles/pixel, cutoff strength: 1.8) and an FDK back-projection [11]. Reconstructions and forward projections were performed using the in-house open-source software framework CONRAD [12].

Reconstructed volumes had 512 x 512 x 400 voxels with an isotropic spacing of 0.5 mm. The uncompensated reconstruction was convolved with a Gaussian kernel having an isotropic standard deviation of 1 mm. MIPs of the initial reconstruction were calculated for each geometry, corresponding to the projection $P_i \in P$. Figure 1 shows representative MIPs beneath the corresponding acquired projections. The modeling clay did not disturb the acquired projections (a), (b), and (c), but introduced significant artifacts into the MIPs (d), (e), and (f).

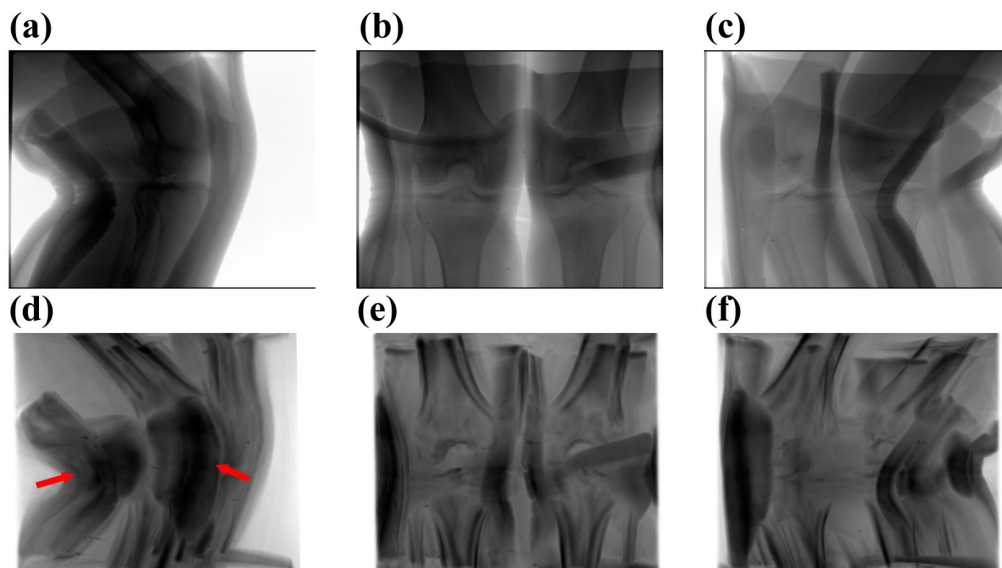


Figure 1. Representative MIPs (d, e, f) beneath the corresponding projections (a, b, c) at different geometries for the scan with the largest involuntary motion. Note the strong contributions of the modeling clay in the MIPs (d, e, f). Representative manifestations of such artifacts are indicated by the arrows (d).

A multi-scale registration is used to obtain the 2D projection shifts for each projection $P_i \in P$. The registration is driven by the maximization of mutual information [13] using a gradient-descent-type optimizer. A formal definition of mutual information assuming a transformation $T(x)$ of locations x is given in Eq. (1):

$$I(m(x), f(T(x))) = h(m(x)) + h(f(T(x))) - h(m(x), f(T(x))), \quad (1)$$

where m and f are the fixed and moving images, and h is either the entropy of a random variable or the joint entropy:

$$h(y) = - \int p(y) \ln(p(y)) dy, \quad (2)$$

$$h(y, z) = - \int p(y, z) \ln(p(y, z)) dz dy. \quad (3)$$

The probability density functions $p(y)$ are approximated using Parzen Windows [13]. The quality of such estimates depends on the proper selection of the underlying density. We use Gaussian densities [13], making the registration susceptible to the choice of standard deviations. Four scale space levels were used. The resulting 2D shifts were smoothed with an averaging kernel to compensate for improbable registration results. The smoothed shifts were applied to the data, and the motion-compensated reconstruction was calculated using the procedure summarized above. We use the 2D projection shifts calculated using the marker-based method as a gold standard for the evaluation of our new method.

3. RESULTS

Figure 2 and Figure 3 show the 2D projection shifts obtained using the fiducial marker-based method [2] and the proposed image-based method for the scans with the second-largest and the largest involuntary motion, respectively. For the scan with the second-largest involuntary motion, the new image-based method resulted in an average error of 2.89 mm +/- 1.24 mm with respect to the marker-based analysis, whereas no correction at all would result in a mean error of 3.50 mm +/- 1.90 mm. For the scan containing the largest motion, the image-based method performed slightly better resulting in an average error of 2.90 mm +/- 1.43 mm, compared to a mean error of 4.10 mm +/- 3.03 mm in the uncorrected case. The modeling clay, used to avoid detector saturation, introduced significant high-contrast structures in the MIP, resulting in a less stable registration problem. We expect more consistent results for projection images acquired without modeling clay, as this would increase the dominance of bony structures in the MIP.

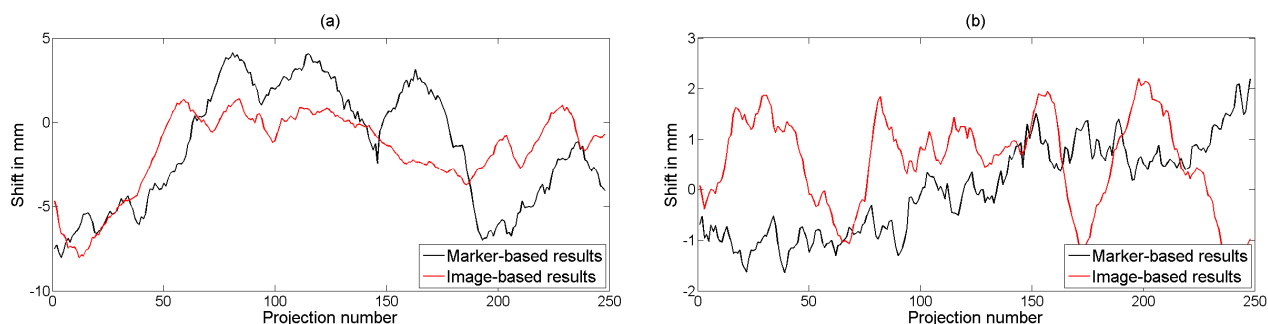


Figure 2. 2D projection shifts for the scan with the second-largest involuntary motion in direction of detector u- and v-coordinate in image (a) and (b), respectively.

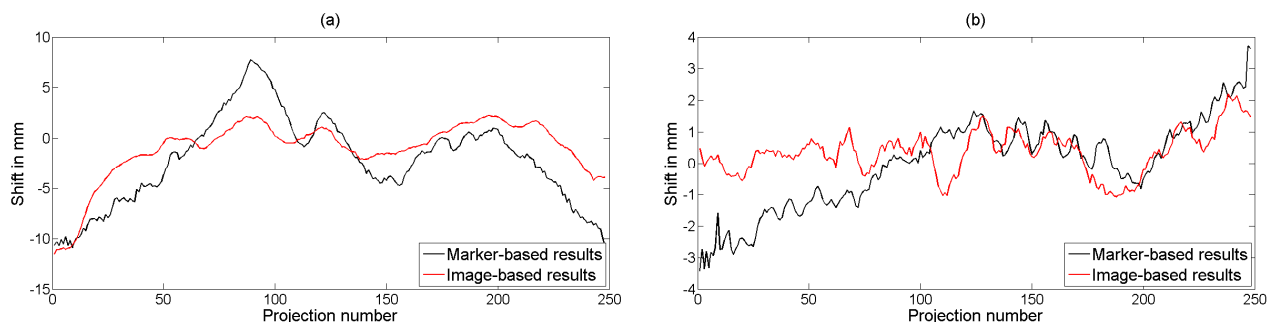


Figure 3. 2D projection shifts for the scan with the largest involuntary motion in direction of detector u- and v-coordinate in image (a) and (b), respectively.

Figure 4 and Figure 5 show representative reconstructed slices of the scan with the second-largest motion and the largest motion, respectively. We show slices below (a and b) and above (c and d) the knee joint, where images (a and c) were reconstructed using the proposed method and images (b and d) were reconstructed without motion compensation. An increase in continuity of the layer of modeling clay is apparent in both cases, and slight improvements of the bones' delineation can be observed. The registration is tuned for bone-alignment. Large contributions of the modeling clay to the MIP, however, change the dominant features in the projections from bones to clay structures, leading to an unstable registration or unfavorable results. Slices from the scan with the largest motion above (bottom row) and below (top row) the knee joint obtained with an uncompensated reconstruction (a and d), the proposed image-based 2D projection-shift approach (b and e), and the marker-based 2D projection-shift method (c and f) are shown in Figure 6. In agreement with the quantitative errors calculated earlier, the proposed method ($2.90 \text{ mm} \pm 1.43 \text{ mm}$) showed improved image quality over the uncompensated method ($4.10 \text{ mm} \pm 3.03 \text{ mm}$), but was not able to outperform the marker-based approach.

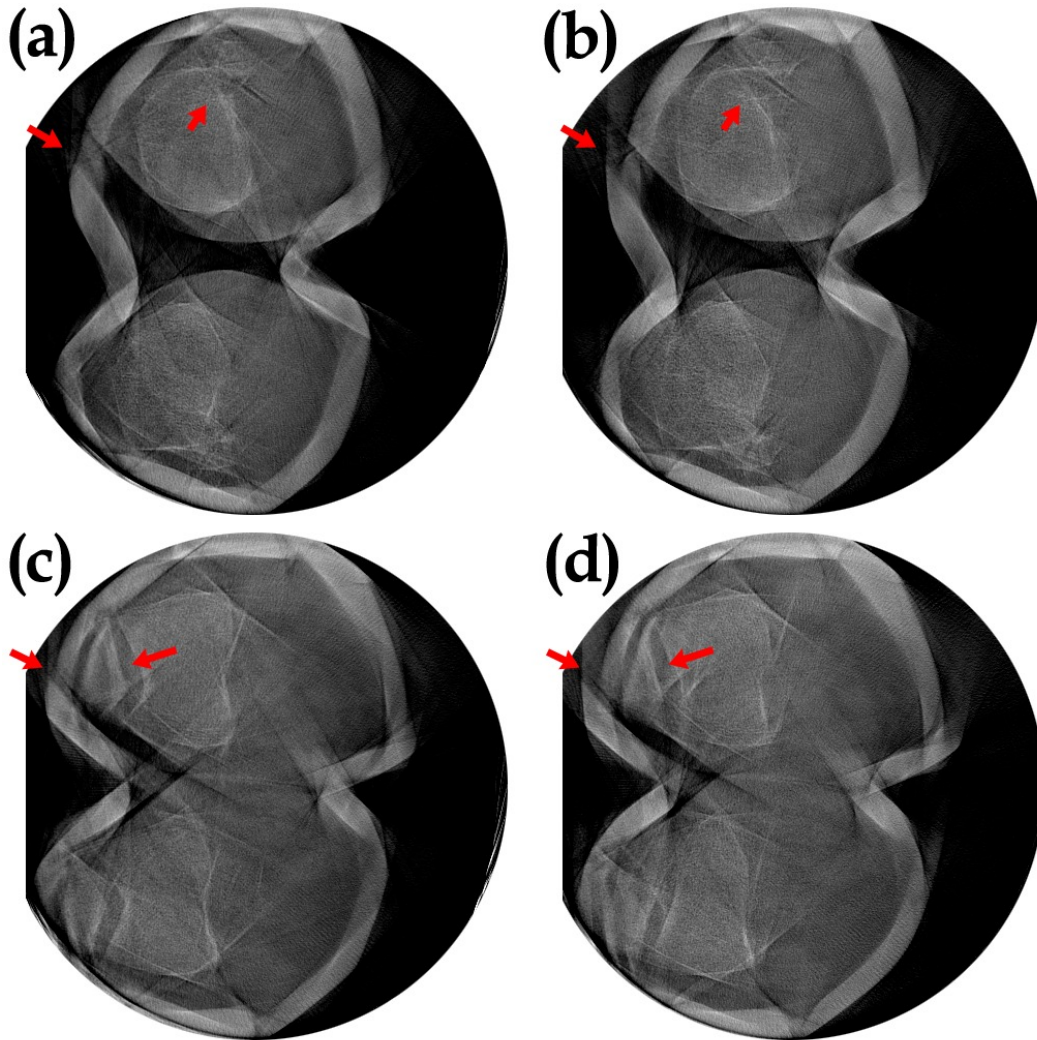


Figure 4. Representative slices of the reconstructed scan with the second-largest motion using the proposed method (a, c) and an uncorrected reconstruction (b, d). The arrows indicate improvements in the continuity of the modeling clay layer and the delineation of the tibia, and patella.

4. DISCUSSION

Previous motion-compensation algorithms used fiducial markers to estimate the static mean positions of the marker attachment points in 3D. Next, the marker locations were forward projected and compared to the measured marker location yielding a 2D shift for each projection [1].

The proposed method bypasses the need for fiducial markers by relying on several assumptions. First, the motion has to be visible in the high-intensity structures of the reconstruction, because only those structures will be prominent in the maximum intensity forward projections. Although bones are usually visible in MIPs, large contributions of other structures (such as modeling clay) to the MIPs may bias the registration towards alignment of those structures. Consequently, the resulting projection shifts will not be optimized, if the dominant structures in the MIPs do not follow the same motion as the bones. This behavior can be observed in Figure 4 and Figure 5, where the layer of modeling clay shows increased continuity but bone contour contrast improves only slightly.

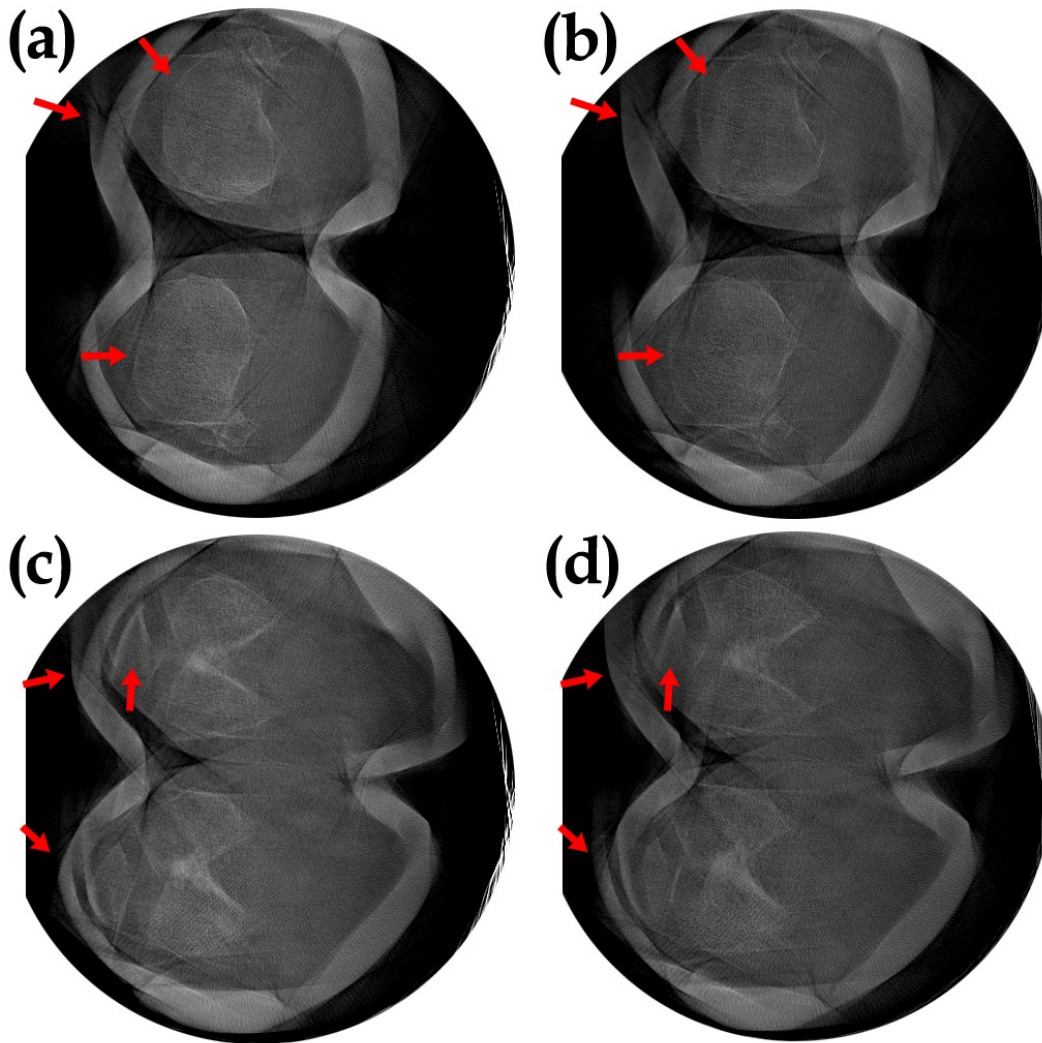


Figure 5. Representative slices of the compensated (a, c) and the uncorrected reconstruction (b, d) of the scan with the largest involuntary motion. The arrows indicate improvements in the continuity of the modeling clay layer and the delineation of the tibia, femur, and patella.

MIPs have been employed successfully in the context of motion-compensated reconstruction of coronary arteries. However, segmentation of the structures of interest in projection- and reconstruction-space (before maximum intensity forward projection) is imperative, to allow for stable registration of segmented images [14]. The proposed method for involuntary motion compensation during the scanning of knees does not require segmentation but therefore results in a more challenging registration problem. Simultaneous scanning of both knees allows for short examination times. However, due to the overlap at certain viewing angles, it gives rise to edges and regions of higher attenuation that are not reproducible in MIPs and result in dissimilar histograms. Therefore, it may be advantageous to replace the maximum intensity forward projections with standard, integrating forward projections of the initial reconstruction. However, this is not possible with filtered-back-projection type reconstruction strategies due to ramp-filtering. It would require more complex reconstruction methods, such as total-variation regularized iterative reconstruction [15].

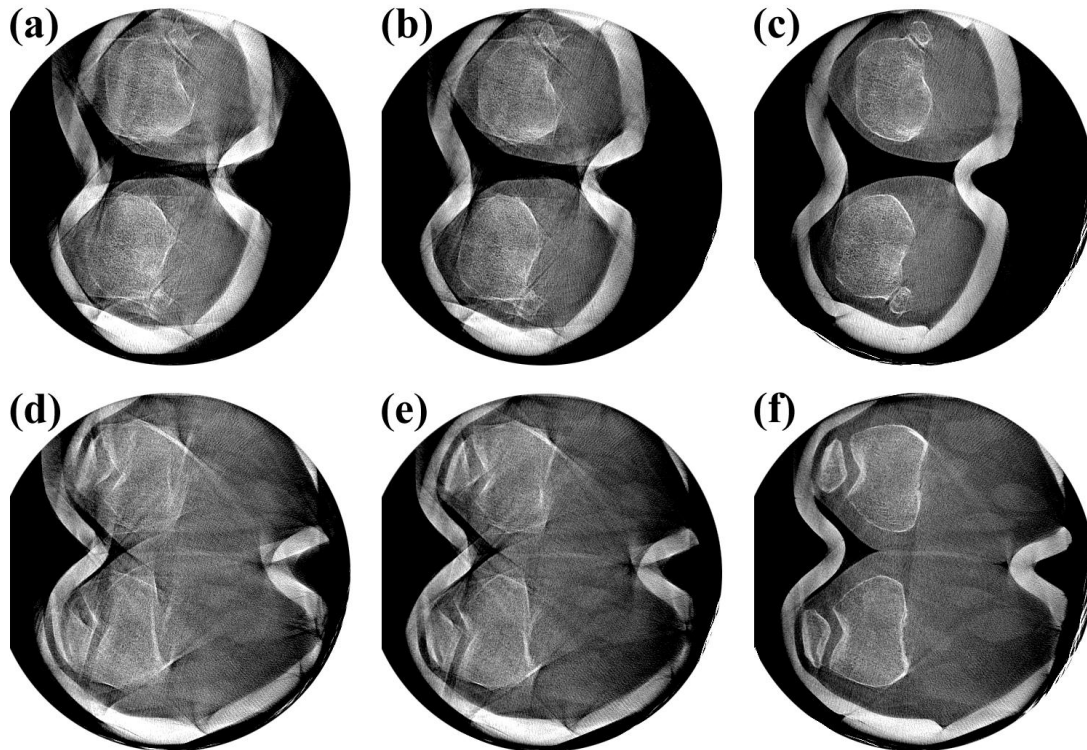


Figure 6. Slices from the reconstruction of the scan with the largest motion below (top row) and above (bottom row) the knee joint. The reconstruction was performed with an uncompensated method (a and d), the proposed image-based method (b and e), and the marker-based projection-shift method (c and f).

5. CONCLUSIONS

Marker-based motion-compensation algorithms significantly reduce motion-related artifacts in reconstructed images but lead to increased examination times and patient discomfort due to the marker attachment process. The proposed image-based 2D projection shifting approach is able to model the general trend of the effects of involuntary motion on the projection. We observed improvements in the reconstruction that manifested in an improved continuity of the modeling clay around the patient's knees and increased visibility of the bone's delineation. This initial investigation suggests that this method performs best for large motions, and less prominent non-bone contributions to the MIPs. The method may benefit from the use of regularized iterative reconstruction followed by standard forward projections instead of MIPs in order to obtain more similar images for registration. This work is a first step towards automatic image-based compensation for involuntary motion in weight-bearing CT scanning of knees. Future work could focus on modeling involuntary motion in 3D using 2D-3D registration. Due to dissimilar histograms of MIPs and original projections, stable registration remains challenging.

ACKNOWLEDGEMENTS

This work was supported by NIH 1 R01HL087917, Siemens Medical Solutions, the Lucas Foundation, CBIS (Center for Biomedical Imaging at Stanford) Seed Funding and the Research Training Group 1773 "Heterogeneous Image Systems", funded by the German Research Foundation (DFG). This work was never submitted, published, or presented before.

REFERENCES

- [1] Choi, J.-H., Fahrig, R., Keil, A., Besier, T. F., Pal, S., McWalter, E. J., Beaupré, G. S. and Maier, A., "Fiducial marker-based correction for involuntary motion in weight-bearing C-arm CT scanning of knees. Part I. Numerical model-based optimization, " *Medical Physics* 40(9), 091905, (2013).
- [2] Maier, A., Choi, J.-H., Keil, A., Niebler, C., Sarmiento, M., Fieselmann, A., Gold, G., Delp, S. and Fahrig, R., "Analysis of vertical and horizontal circular C-arm trajectories," *Proc SPIE*, Lake Buena Vista, Florida, 796123-8, (2011).
- [3] Powers, C. M., Ward, S. R., Fredericson, M., Guillet, M. and Shellock, F. G., "Patellofemoral kinematics during weight-bearing and non-weight-bearing knee extension in persons with lateral subluxation of the patella: a preliminary study," *The Journal of orthopaedic and sports physical therapy*, 33(11), 677-85, (2003).
- [4] Choi, J.-H., Maier, A., Keil, A., Pal, S., McWalter, E. J., Beaupré, G. S., Gold, G. E. and Fahrig, R., "Fiducial Marker-based Correction for Involuntary Motion in Weight-bearing C-arm CT Scanning of Knees. Part II. Experiment, " *Medical Physics* 41(6), 061902, (2013).
- [5] Schwemmer, C., "High-Density Object Removal from X-ray Projection Images," Master's Thesis, 65-67, Universität Erlangen-Nürnberg, Germany, (2010)
- [6] Zellerhoff, M., Scholz, B., Ruehrnschopf, E. P., Brunner, T., "Low contrast 3D reconstruction from C-arm data," *Medical Imaging 2005: Physics of Medical Imaging*, Proceedings of SPIE 5745:646-655, (2005).
- [7] Dragusin, O., Bosmans, H., Pappas, C., Desmet, W., "An investigation of flat panel equipment variables on image quality with a dedicated cardiac phantom," *Phys. Med. Biol.* 53:4927-40, (2008).
- [8] Kak, A. C., Slaney, M., "Principles of Computerized Tomographic Imaging," IEEE Service Center, Piscataway, NJ, United States, (1988).
- [9] Parker, D. L., "Optimal short scan convolution reconstruction for fanbeam CT," *Medical Physics*, 9(2), 254-7, (1982).
- [10] Ohnesorge, B., Flohr, T., Schwarz, K., Heiken, J. P., Bae, K. T., "Efficient correction for CT image artifacts caused by objects extending outside the scan field of view," *Medical Physics*, 27(1), 39-46, (2000).
- [11] Feldkamp, L. A., Davis, L. C. and Kress, J. W., "Practical Cone-Beam Algorithm," *Journal of the Optical Society of America*, 1(6), 612-619, (1984).
- [12] Maier, A., Hofmann, H. G., Berger, M., Fischer, P., Schwemmer, C., Wu, H., Muller, K., Hornegger, J., Choi, J. H., Riess, C., Keil, A. and Fahrig, R., "CONRAD-A software framework for cone-beam imaging in radiology, " *Med Phys*, 40(11), 111914, (2013).
- [13] Viola, P., Wells III, W. M., "Alignment by maximization of mutual information," *International journal of computer vision*, 24(2), 137-154, (1997).
- [14] Schwemmer, C., Rohkohl, C., Lauritsch, G., Müller, K. and Fahrig, R., "Residual motion compensation in ECG-gated cardiac vasculature reconstruction," *Proceedings of the Second International Conference on Image Formation in X-ray Computed Tomography*, edited by Noo, F. (University of Utah, Salt Lake City, Utah, 2012), 259-262, (2012)
- [15] Sidky E. Y., Pan, X., "Image reconstruction in circular cone-beam computed tomography by constrained, total-variation minimization," *Physics in Medicine and Biology*, 53(17), 4777, (2008)